

Impact of Rates of Change of Lamina Cribrosa and Optic Nerve Head Surface Depths on Visual Field Progression in Glaucoma

Zhongheng Wu,¹ Chen Lin,¹ Michael Crowther,² Heather Mak,¹ Marco Yu,³ and Christopher K.-S. Leung¹

¹Department of Ophthalmology and Visual Sciences, The Chinese University of Hong Kong, Hong Kong, People's Republic of China

²Department of Health Sciences, College of Medicine, Biological Sciences and Psychology, University of Leicester, Leicester, United Kingdom

³Department of Mathematics and Statistics, Hang Seng Management College, Hong Kong, Hong Kong, People's Republic of China

Correspondence: Christopher K.-S. Leung, Department of Ophthalmology and Visual Sciences, The Chinese University of Hong Kong, 147K Argyle Street, Hong Kong Eye Hospital, Hong Kong, People's Republic of China; tlims00@hotmail.com.

ZW and CL contributed equally to the work presented here and should therefore be regarded as equivalent authors.

Submitted: August 11, 2016

Accepted: December 21, 2016

Citation: Wu Z, Lin C, Crowther M, Mak H, Yu M, Leung CK-S. Impact of rates of change of lamina cribrosa and optic nerve head surface depths on visual field progression in glaucoma. *Invest Ophthalmol Vis Sci*. 2017;58:1825-1833. DOI:10.1167/iov.16-20509

PURPOSE. To investigate the impact of the rates of change of anterior lamina cribrosa surface depth (ALCSD) and optic nerve head surface depth (ONHSD) on visual field (VF) progression in glaucoma.

METHODS. One hundred forty-six eyes of 95 glaucoma patients had optical coherence tomography ONH imaging and VF testing at approximately 4-month intervals for greater than or equal to 5 years. Anterior lamina cribrosa surface depth and ONHSD were measured with reference to (1) Bruch's membrane opening (BMO), and (2) choroid-sclera interface (CSI). The rates of change of ALCSD and ONHSD of individual eyes were measured with linear regression analysis. The hazard ratios (HRs) of the rates of change of ALCSD/ONHSD for prediction of VF progression as per Early Manifest Glaucoma Trial criteria were determined by joint longitudinal and survival models.

RESULTS. Using the BMO reference, 23.3% and 28.1% of eyes showed a significant positive trend (posterior displacement), whereas 29.5% and 24.0% showed a significant negative trend (anterior displacement) of ALCSD and ONHSD, respectively. Using the CSI reference, the proportions with a significant negative trend decreased to 11.6% and 14.4%, respectively; and the proportions with a significant positive trend increased to 37.7% and 38.4%, respectively. The HRs of VF progression were 1.06 and 1.11 for each micrometer per year increase in the rates of change of ALCSD_{BMO} and ONHSD_{BMO}, respectively; and 1.07 and 1.09 for each micrometer per year increase in the rates of change of ALCSD_{CSI} and ONHSD_{CSI}, respectively.

CONCLUSIONS. Identifying fast progressors of posterior ALCS/ONHS displacement is relevant to the management of glaucoma patients as they have a higher risk of VF progression.

Keywords: optic nerve head surface depth, anterior lamina cribrosa surface depth, optical coherence tomography

Optic nerve head (ONH) deformation is a defining feature of glaucoma. While confocal scanning laser ophthalmoscopy (CSLO) and optical coherence tomography (OCT) have been widely adopted for measurement of the neuroretinal rim,¹⁻⁶ parameters like anterior lamina cribrosa surface depth (ALCSD) and ONH surface depth (ONHSD) are rarely examined in clinical practice. Studies reporting long-term, progressive LC and ONH surface deformation in glaucoma patients are sparse. We previously investigated the longitudinal changes of ALCSD and ONHSD in glaucoma patients with reference to Bruch's membrane opening (BMO) using an event analysis.⁷ However, event analysis cannot reveal how fast an individual eye is progressing. The rates of change of ALCSD and ONHSD over the course of glaucoma progression have not been reported. The significance of measurement of LC and ONH deformation in the management of glaucoma patients remains unclear.

Studies in nonhuman primates suggest deformation of the LC and the ONH surface to be detectable prior to axonal damage and functional loss of the optic nerve in experimental glaucoma.^{8,9} We hypothesize that progressive posterior displacement

of the LC and the ONH surface is indicative of an increased stress to the optic nerve and that individuals with a faster rate of posterior displacement of the anterior LC surface and the ONH surface entail a higher risk of development of visual field (VF) progression. In this prospective study, we imaged the ONH with OCT and measured the rates of change of ALCSD and ONHSD with reference to (1) the Bruch's membrane opening (BMO), and (2) the choroid-sclera interface (CSI) in 146 eyes of 95 glaucoma patients who were monitored at approximately 4-month intervals for greater than or equal to 5 years with an objective of investigating the impact of the rates of change of ALCSD and ONHSD on the risk of development of VF progression.

METHODS

Subjects

One hundred forty-six eyes of 95 glaucoma patients from the Optic Nerve Head Deformation in Glaucoma Study, a prospective



study series investigating the longitudinal profiles of LC and ONH displacement in glaucoma, were analyzed. They were consecutively recruited and followed-up at approximately 4-month intervals from March 2008 to September 2015 at the University Eye Center, the Chinese University of Hong Kong. All patients had a complete ocular examination including measurement of visual acuity, IOP (dynamic contour tonometry), axial length (A-scan), and refraction. Color optic disc stereophotographs were taken with a fundus camera (TRC-50DX; Topcon, Tokyo, Japan). Eyes included in the study had visual acuity greater than or equal to 20/40 and had longitudinal follow-up greater than or equal to 5 years. Eyes were excluded if there was evidence of macular disease, neurologic disease, or refractive or retinal surgery. Glaucoma was diagnosed by characteristic optic disc/retinal nerve fiber layer (RNFL) changes (i.e., optic disc excavation/narrowed neuroretinal rim/RNFL defects) in color optic disc stereophotographs with corresponding VF abnormalities in at least one eye, independent of the level of IOP. At the 4-monthly follow-up visits, both eyes were examined under slit-lamp biomicroscopy with IOP measured with dynamic contour tonometry (DCT; the average of two diastolic IOP measurements with a quality score between 1 and 3 was recorded),¹⁰⁻¹² ONH imaged with OCT, and VF measured with standard automated white-on-white perimetry (described below). Patients were managed at the discretion of the attending ophthalmologists without taking consideration of OCT analysis of the anterior LC and the ONH surfaces. The study was conducted in accordance with the ethical standards stated in the 1964 Declaration of Helsinki and approved by the local research ethics committee with informed consent obtained.

Optical Coherence Tomography Imaging

The ONH was imaged with the Spectralis OCT (Heidelberg Engineering, Heidelberg, Germany). The scan protocol comprised 6 radial scan lines, each with 1024 A-scans equally spaced at 30° centered at the ONH with reference to the operator estimation of the clinically visible optic disc margin. Automatic image averaging was performed with 15 B-scans for each radial scan line. Follow-up scans were obtained at the same locations of the registered baseline visit using the eye-tracking function. All OCT volumes had a scan quality score of greater than or equal to 20. As the study was initiated before the availability of enhanced-depth imaging (EDI),¹³ only non-EDI baseline and follow-up scans with clear visibility of the anterior LC and the ONH surfaces were included in the analysis. After excluding 13 eyes of 13 glaucoma patients because of indiscernible anterior LC surface in at least one B-scan in the baseline and follow-up visits (i.e., all included eyes had 6 B-scans in each visit for analysis), 146 eyes of 95 glaucoma patients were analyzed. There were no significant differences in age, sex, IOP, axial length, central corneal thickness, average RNFL thickness, VF mean deviation (MD), and ONHSD measured at the baseline visit between the excluded and included eyes (Supplementary Table S1).

Measurement of ALCSO and ONHSD

Optical coherence tomography B-scans (1:1 pixel in scale) were exported as image files after setting the baseline as reference. The ALCSO and ONHSD were measured with reference to the axial and transverse scaling factors (μm/pixel) of individual B-scans as reported in the Spectralis OCT operating system. Images were analyzed in a computer using a customized program developed in Matlab (R2010a; The MathWorks, Inc., Natick, MA, USA). Two anatomical landmarks (1) the Bruch's membrane opening (BMO) and (2) the choroid-sclera interface (CSI) were referenced for measurements of

ALCSO and ONHSD (Fig. 1). $ALCSO_{BMO}$ and $ONHSD_{BMO}$ were measured after the BMO reference line (a line joining the BMO in a B-scan), the internal limiting membrane, and the anterior LC and the ONH surfaces were manually located (assisted by the piecewise cubic Hermite interpolation polynomial). $ALCSO_{CSI}$ and $ONHSD_{CSI}$ were measured with reference to the CSI reference line. The CSI reference line was a line joined by the CSI located between 1700 and 1800 μm from the BMO central axis point.¹⁴ The CSI positions were marked along the 1700- to 1800-μm distance from the BMO central axis point to minimize errors associated with focal fluctuations of the CSI.¹⁴ The $ALCSO_{BMO}$ and $ALCSO_{CSI}$ were defined as the perpendicular distances from the BMO and CSI reference lines, respectively, to the detectable anterior LC surface, which was visualized as the interface bordering the prelaminar tissue (moderate-intensity signal below the ONH surface) and the LC (high-intensity vertical striations; Fig. 1C).^{5,7} $ONHSD_{BMO}$ and $ONHSD_{CSI}$ were defined as the perpendicular distances from the BMO and CSI reference lines, respectively, to the ONH surface (Fig. 1D). The ALCSO and ONHSD of an eye were measured as the averages of the six radial B-scans. To account for the fact that the radial scan pattern under-represented the peripheral compared with the central ONH in the measurement of ALCSO and ONHSD (the OCT sampling density was higher near the optic disc center than the peripheral), each of the delineated distances at the anterior LC and ONH surfaces was weighted in proportion to its distance from the center point between the pair of BMO points using the formulas:

$$\bar{y} = \frac{\sum_{i=1}^6 \bar{y}_i}{6} \quad (1)$$

$$\bar{y}_i = \frac{\sum_{j=1}^{n_i} d_{ij} y_{ij}}{\sum_{j=1}^{n_i} d_{ij}} \quad (2)$$

where \bar{y} represents the mean ALCSO/ONHSD of an eye, which is given by averaging the mean values of each of the 6 radial B-scans \bar{y}_i (for $i = 1, 2, \dots, 6$). \bar{y}_i represents the weighted average of the distance measure y_{ij} , which is the distance at point j in B-scan i with a weighting given by its distance from the BMO center point, d_{ij} .

Visual Field Examination and Progression Analysis

Standard white-on-white automated perimetry (SITA standard 24-2) was performed using the Humphrey Field Analyzer II-i (Carl Zeiss Meditec, Dublin, CA, USA). Included VF tests had fixation losses and false positive less than or equal to 20%. A VF defect had greater than or equal to three nonedge contiguous locations with $P < 0.05$ (≥ 1 location with $P < 0.01$) on the same side of horizontal meridian in the pattern deviation plot confirmed with greater than or equal to two consecutive examinations. Visual field progression was analyzed using the Early Manifest Glaucoma Trial (EMGT) criteria.¹⁵ Visual field progression was defined when greater than or equal to three locations had a significant change compared with two baseline examinations (separated by ~4 months) for at least three consecutive visits (i.e., "likely progression" reported in the Guided Progression Analysis).

Statistical Analysis

Statistical analyses were performed with Stata (ver. 14.0; StataCorp., College Station, TX, USA). The rates of change of ALCSO and ONHSD of individual eyes were calculated with

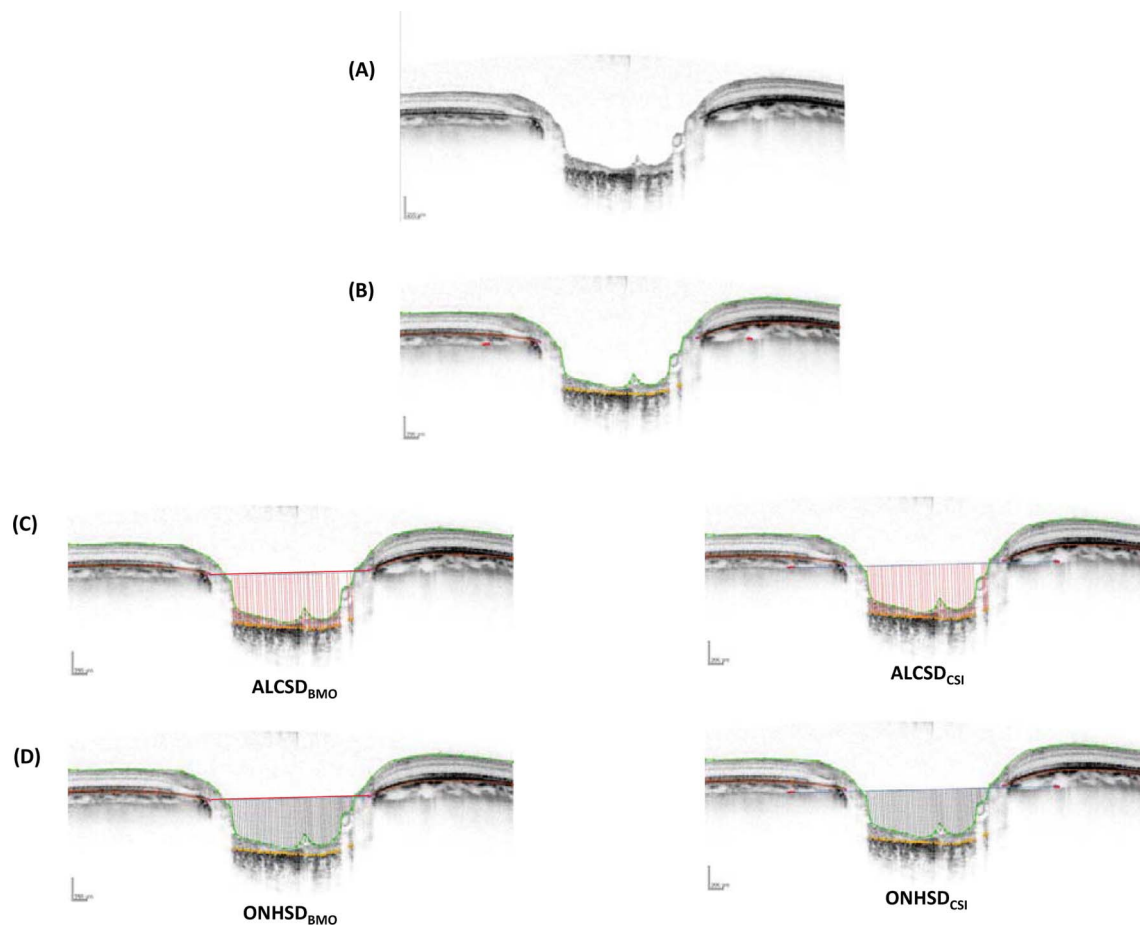


FIGURE 1. Measurements of ALCS and ONHSD. An OCT B-scan image of a glaucomatous eye (A) before and (B) after manual detection of the BMO (pink dots), the CSI between 1700 and 1800 μm from the BMO central axis point (red dots), the internal limiting membrane/ONH surface (green), and the anterior LC surface (orange). (C) The ALCS represents the perpendicular distances from the BMO reference line (red; left panel) or CSI reference line (blue; right panel) to the detectable anterior LC surface. The BMO reference line is a line joined by the BMO. The CSI reference line was a line joined by the CSI located between 1700 and 1800 μm from the BMO central axis point. (D) The ONHSD represents the perpendicular distances from the BMO reference line (left panel) or the CSI reference line (right panel) to the ONH surface (the black lines are for illustrative purpose and do not represent all the lines the software measured).

linear regression analysis between ALCS/ONHSD and time. Multilevel linear mixed-modeling was applied to identify factors associated with the rates of change of ALCS and ONHSD. Time (follow-up duration at each follow-up visit), baseline age, baseline axial length, baseline central corneal thickness, baseline ALCS/ONHSD, IOP during follow-up, and the interactions between the baseline covariates and time were included in the linear mixed-models as fixed effects with random intercepts and random slopes allowing different baseline ALCS/ONHSD values and different rates of change of ALCS/ONHSD for individual eyes. Normality assumption of the random effects in the linear mixed-models (i.e., rates of change of ALCS/ONHSD of individual eyes) was checked (Supplementary Fig. S1). The HRs of the rates of change of ALCS/ONHSD and other biometric variables for prediction of VF progression were computed with joint longitudinal and survival modeling with ALCS/ONHSD measurements nested in eyes. The application of joint longitudinal and survival modeling was initially described by Faucett and Thomas.¹⁶ It has two components: (1) a longitudinal submodel and (2) a survival submodel. In this study, the trajectory function of ALCS/ONHSD and the covariates were fitted using linear mixed-modeling in the longitudinal submodel. The estimates of the coefficients in the linear mixed-model and the first derivative of the trajectory function of ALCS/ONHSD (i.e.,

the rates of change of ALCS/ONHSD) were then carried forward to a proportional hazards survival model specified by a Weibull distribution in the survival submodel. Anterior lamina cribrosa surface depth and ONHSD were separately analyzed in the joint models. Model fitting and conditional VF survival predictions for individual eyes were performed using the Stata

TABLE 1. Demographics and Biometric Variable Measured at the Baseline Visit

Biometric Variables	Mean \pm SD (Range)
Eye/patients	146/95
Age, y	49.9 \pm 15.0 (17 to 84)
Male/female	51/44
Axial length, mm	25.23 \pm 1.91 (21.81 to 30.10)
Central corneal thickness, μm	545.7 \pm 35.5 (406 to 623)
IOP, mm Hg	18.7 \pm 2.8 (10.1 to 34.8)
ALCS _{BMO} , μm	452.2 \pm 101.7 (224.3 to 723.7)
ONHSD _{BMO} , μm	246.4 \pm 87.2 (59.7 to 517.2)
ALCS _{CSI} , μm	419.6 \pm 101.9 (218.8 to 697.0)
ONHSD _{CSI} , μm	256.1 \pm 95.9 (20.6 to 496.2)
Average RNFL thickness, μm	66.6 \pm 17.2 (30 to 108)
VF MD, db	-9.53 \pm 9.00 (-32.81 to 0.37)

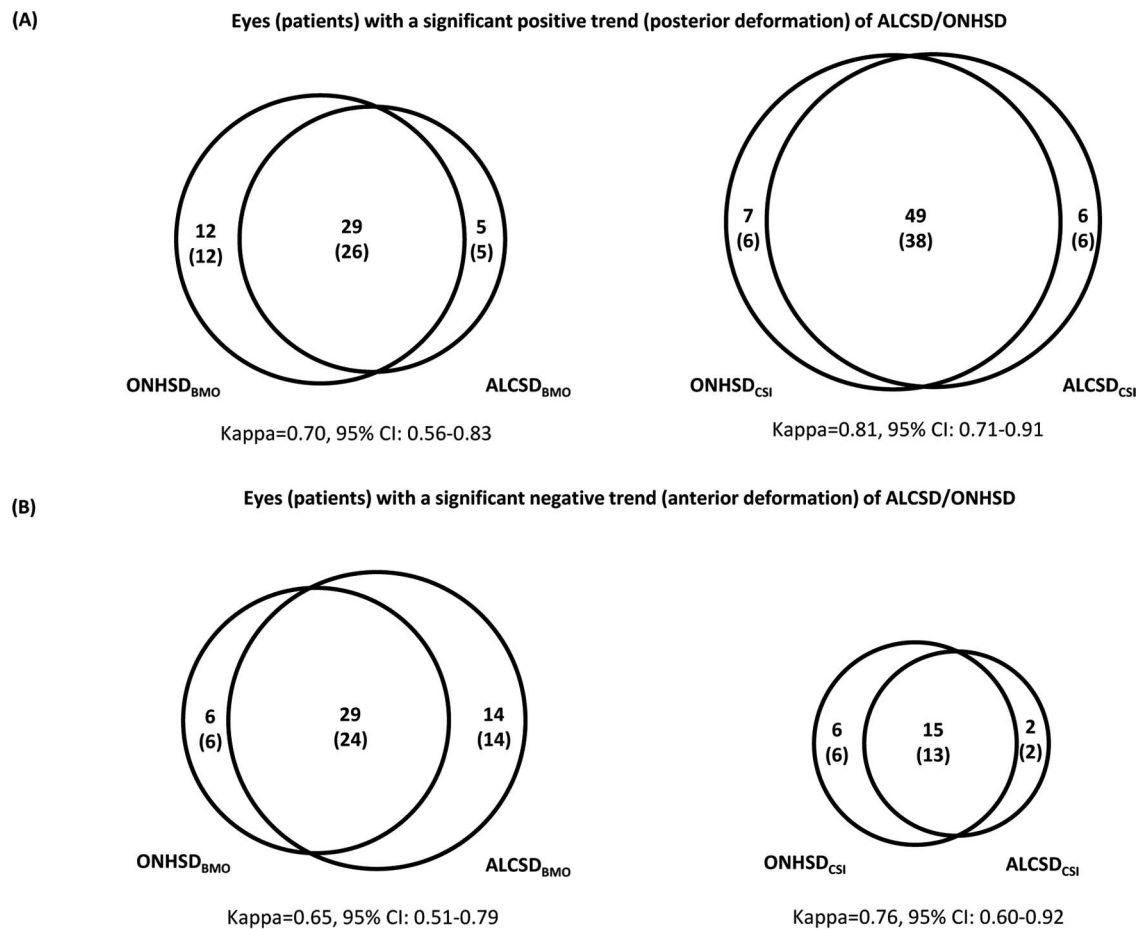


FIGURE 2. Agreement between anterior ALCSO and ONHSD. Venn diagrams showing the number of eyes (the number of patients in parentheses) with significant (A) posterior and (B) anterior displacement of the anterior lamina cribrosa surface and the ONH surface (determined by linear regression analysis between ALCSO/ONHSD and time) measured with reference to the BMO (*left panel*) and the CSI (*right panel*).

codes developed by Crowther.¹⁷ *P* value less than 0.05 was considered statistically significant.

RESULTS

Table 1 shows the demographics of the 146 eyes of 95 glaucoma patients. The mean follow-up duration was 6.5 years (range, 5.0–7.4 years) and the mean number of follow-up visits for each patient was 17.3 (range, 8–21 visits). A total of 15,144 B-scans (6 B-scans for each eye \times 146 eyes \times 17.2877 visits) were segmented and analyzed. At the baseline, 49.3% of eyes had VF MD greater than or equal to -6 dB, 22.6% had VF MD between -6 and -12 dB, and 28.1% had VF MD less than or equal to -12 dB. Fourteen eyes (9.6%) showed “likely” VF progression during the study follow-up.

Rates of Change of ALCSO and ONHSD – Linear Regression Analysis

Using linear regression analysis to measure the rates of change of ALCSO_{BMO} and ONHSD_{BMO} in individual eyes, 23.3% (34 eyes) and 28.1% (41 eyes) eyes showed a significant ($P < 0.05$) positive trend, respectively (i.e., posterior LC/ONH surface displacement); whereas 29.5% (43 eyes) and 24.0% (35 eyes) showed a significant negative trend, respectively (i.e., anterior LC/ONH surface displacement; Fig. 2). For eyes with a significant positive trend, the rates of change of ALCSO_{BMO}

and ONHSD_{BMO} ranged from 1.3 to 23.3 $\mu\text{m}/\text{year}$, and from 1.4 to 29.0 $\mu\text{m}/\text{year}$, respectively (Fig. 3A). For eyes with a significant negative trend, they ranged from -1.7 to $-21.0 \mu\text{m}/\text{year}$, and from -1.3 to $-12.8 \mu\text{m}/\text{year}$, respectively.

Using the CSI reference, the proportions of eyes with a significant positive trend of ALCSO_{CSI} and ONHSD_{CSI} increased to 37.7% (55 eyes) and 38.4% (56 eyes), respectively ($P \leq 0.010$); and the proportion of eyes with a significant negative trend decreased to 11.6% (17 eyes) and 14.4% (21 eyes), respectively ($P \leq 0.001$; Fig. 2). The rates of change of ALCSO_{CSI} and ONHSD_{CSI} ranged from 1.2 to 26.3 $\mu\text{m}/\text{year}$, and from 1.2 to 34.8 $\mu\text{m}/\text{year}$, respectively, for eyes with a significant positive trend; and from -1.8 to $-26.3 \mu\text{m}/\text{year}$, and from -1.3 to $-17.6 \mu\text{m}/\text{year}$, respectively, for eyes with a significant negative trend (Fig. 3B).

Determinants of the Rates of Change of ALCSO and ONHSD – Linear Mixed Modeling

Baseline ALCSO/ONHSD, baseline age, and IOP during follow-up ($P \leq 0.015$), but not baseline axial length, baseline CCT, and baseline VF MD ($P \geq 0.122$), were associated with the rates of change of ALCSO and ONHSD measured with reference to the BMO (Table 2) and the CSI (Table 3). Intraocular pressure during follow-up was positively, whereas age and ALCSO/ONHSD at the baseline were negatively associated with the rates of change of ALCSO and ONHSD.

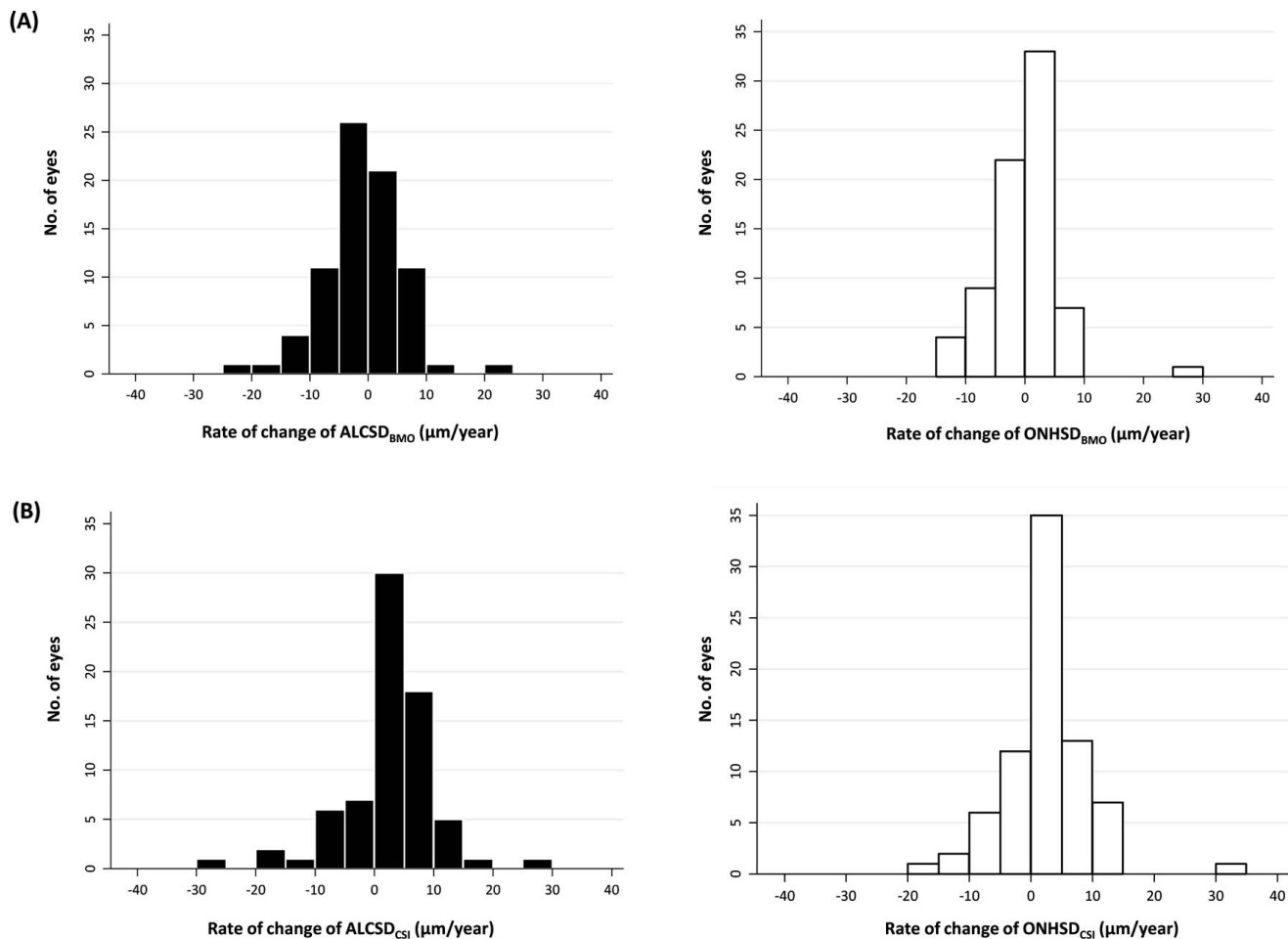


FIGURE 3. Rates of change of ALCSDBMO and the ONHSD. Frequency distribution plots of the rates of change of ALCSDBMO (left panel) and ONHSD_BMO (right panel) in eyes with significant ($P < 0.05$) positive or negative trends of ALCSDBMO/ONHSD measured with reference to (A) the BMO and (B) the CSI.

Impact of Rates of Change of ALCSDBMO and ONHSD on VF Progression – Joint Longitudinal and Survival Modeling

The rates of change of ALCSDBMO and ONHSD were significantly associated with the risk of VF progression after controlling for baseline age, baseline ALCSDBMO/ONHSD, baseline VF MD, and IOP during follow-up, regardless of the reference (BMO/CSI) for measurements of ALCSDBMO/ONHSD (Tables 4, 5). The HR of VF progression were 1.06 (95% confidence interval [CI]: 1.01–

1.12) and 1.11 (95% CI: 1.02–1.21) for each micrometer per year increase in the rates of change of ALCSDBMO and ONHSD_BMO, respectively (Table 4); and 1.07 (95% CI: 1.02–1.14) and 1.09 (95% CI: 1.01–1.18) for each micrometer per year increase in the rates of change of ALCSDCSI and ONHSD_CSI, respectively (Table 5). Baseline age, baseline ALCSDBMO/ONHSD, baseline VF MD, and IOP during follow-up were not associated with VF progression ($P \geq 0.414$). The rates of change of maximum ALCSDBMO/maximum ONHSD (i.e., the mean of the maximum ALCSDBMO/ONHSD measured from each of

TABLE 2. Rates of Change of ALCSDBMO and ONHSD_BMO and Their Determining Factors Analyzed With Multivariable Linear Mixed-Models

Biometric Variables	ALCSDBMO		ONHSD_BMO	
	Coefficient (95% CI)	P Value	Coefficient (95% CI)	P Value
Time, y	7.73 (2.33 to 13.13)	0.005	5.75 (2.22 to 9.27)	0.001
Baseline ALCSDBMO/ONHSD_BMO, μm	0.96 (0.94 to 0.98)	<0.001	0.99 (0.97 to 1.00)	<0.001
Baseline age, y	-0.15 (-0.31 to 0.02)	0.078	-0.04 (-0.14 to 0.07)	0.511
IOP, mm Hg	-0.11 (-0.49 to 0.26)	0.555	0.07 (-0.20 to 0.35)	0.599
Baseline VF MD, dB	-0.04 (-0.28 to 0.19)	0.724	-0.01 (-0.16 to 0.15)	0.919
Time \times baseline ALCSDBMO/ONHSD_BMO	-0.01 (-0.02 to 0.00)	0.009	-0.01 (-0.02 to 0.00)	0.003
Time \times baseline age	-0.11 (-0.16 to -0.05)	<0.001	-0.09 (-0.14 to -0.04)	<0.001
Time \times IOP	0.15 (0.05 to 0.25)	0.003	0.14 (0.07 to 0.22)	<0.001
Time \times baseline VF MD	0.06 (-0.03 to 0.15)	0.165	0.05 (-0.02 to 0.12)	0.185

Axial length and central corneal thickness were not included in the final multivariable models as their association with the rates of change of ALCSDBMO and ONHSD_BMO were not significant ($P \geq 0.264$).

TABLE 3. Rates of Change of ALCSD_{CSI} and ONHSD_{CSI} and Their Determining Factors Analyzed With Multivariable Linear Mixed-Models

Biometric Variables	ALCSD _{CSI}		ONHSD _{CSI}	
	Coefficient (95% CI)	P Value	Coefficient (95% CI)	P Value
Time, y	11.66 (6.68 to 16.64)	<0.001	8.33 (4.42 to 12.23)	<0.001
Baseline ONHSD _{CSI} /ALCSD _{CSI} , μm	0.96 (0.94 to 0.99)	<0.001	0.98 (0.96 to 1.00)	<0.001
Baseline age, y	-0.09 (-0.25 to 0.06)	0.249	-0.07 (-0.19 to 0.05)	0.253
IOP, mm Hg	0.26 (-0.16 to 0.68)	0.229	0.32 (-0.02 to 0.66)	0.061
Baseline VF MD, dB	-0.12 (-0.36 to 0.13)	0.346	-0.08 (-0.27 to 0.10)	0.377
Time \times baseline ONHSD _{CSI} /ALCSD _{CSI}	-0.02 (-0.03 to -0.01)	<0.001	-0.02 (-0.02 to -0.01)	<0.001
Time \times baseline age	-0.08 (-0.15 to -0.02)	0.011	-0.10 (-0.16 to -0.04)	0.001
Time \times IOP	0.14 (0.03 to 0.25)	0.015	0.17 (0.08 to 0.26)	<0.001
Time \times baseline VF MD	0.06 (-0.03 to 0.16)	0.190	0.07 (-0.02 to 0.16)	0.122

Axial length and central corneal thickness were not included in the final multivariable models as their association with the rates of change of ALCSD_{CSI} and ONHSD_{CSI} were not significant ($P \geq 0.641$).

the 6 radial scans of each eye) measured with reference to the BMO/CSI were also predictive of VF progression (Supplementary Tables S2, S3).

Case examples illustrating the application of joint longitudinal and survival modeling to estimate VF survival probability from longitudinal measurements of ALCSD/ONHSD for an individual eye are shown in Figure 4.

DISCUSSION

In this 5-year prospective study, we reported the rates of change of ALCSD and ONHSD and investigated the determinants and consequences of progressive displacement of the anterior LC surface and the ONH surface in glaucoma. With an average of more than 17 longitudinal ALCSD/ONHSD measurements collected from 146 eyes of 95 glaucoma patients followed at regular intervals over 5 years, we showed that the rates of change of ALCSD and ONHSD varied widely in glaucoma patients (Fig. 3) and they were influenced by age, baseline ALCSD/ONHSD, and IOP during follow-up (Tables 2, 3). Further, we examined the impact of the rates of change of ALCSD and ONHSD on prediction of VF progression using joint longitudinal and survival models. The risk of development of VF progression increased by 6.4% (BMO-based measurements) to 7.4% (CSI-based measurements) for each micrometer per year increase in the rate of change of ALCSD, and by 10.9%

(BMO-based measurements) and 9.3% (CSI-based measurements) for each micrometer per year increase in the rate of change of ONHSD after controlling for the covariates (Tables 4, 5). Our finding underscores the importance of monitoring the ALCSD and ONHSD for risk assessment of VF progression in glaucoma patients.

Short-term changes of ALCSD and ONHSD have been investigated after transient IOP elevation with an ophthalmodynamometer¹⁸ or IOP reduction,¹⁹⁻²¹ but studies investigating long-term, progressive deformation of the LC and the ONH surface in glaucoma are sparse. To our knowledge, our data are the first to measure the rates of change of ALCSD and ONHSD and examine their impact on VF progression in glaucoma patients. While 29.5% and 24.0% of eyes exhibited anterior displacement of the anterior LC and the ONH surfaces over 5 years, respectively, when the ALCSD and ONHSD were measured with reference to the BMO, the respective proportions significantly decreased to 11.6% and 14.4% when the ALCSD and ONHSD were measured with reference to the CSI. The differences in the proportions of eyes with significant anterior LC and ONH surface displacement between BMO- and CSI-based measurements could be attributed to age-related²² and/or glaucoma-related reduction of choroidal thickness.²³ Progressive choroidal thinning can engender an appearance of anterior displacement of the LC and the ONH surface with reference to the BMO, which may not be evident when the

TABLE 4. Hazard Ratios of the Rates of Change of ALCSD_{BMO} and ONHSD_{BMO} and the Covariates for Development of VF Progression Analyzed With Joint Longitudinal and Survival Models

Longitudinal Submodel	ALCSD _{BMO}		ONHSD _{BMO}	
	Coefficient (95% CI)	P Value	Coefficient (95% CI)	P Value
Time, y	7.09 (1.98 to 12.2)	0.007	4.98 (1.46 to 8.51)	0.006
Baseline age, y	-0.76 (-1.85 to 0.34)	0.178	0.02 (-0.94 to 0.98)	0.974
IOP, mm Hg	-0.45 (-0.86 to -0.04)	0.033	0.05 (-0.26 to 0.37)	0.733
Baseline VF MD, dB	-1.05 (-2.84 to 0.74)	0.252	-0.76 (-2.33 to 0.8)	0.338
Time \times baseline age	-0.18 (-0.26 to -0.09)	<0.001	-0.11 (-0.17 to -0.06)	<0.001
Time \times IOP	0.18 (0.07 to 0.29)	0.002	0.12 (0.03 to 0.2)	0.008
Time \times baseline VF MD	0.13 (0.00 to 0.27)	0.048	0.09 (0.00 to 0.18)	0.059
Intercept (baseline ALCSD _{BMO} /ONHSD _{BMO})	488.61 (428.56 to 548.65)	<0.001	237.14 (184.8 to 289.49)	<0.001
Survival Submodel	HR (95% CI)	P Value	HR (95% CI)	P Value
Rate of change of ALCSD _{BMO} /ONHSD _{BMO} (each $\mu\text{m}/\text{y}$)	1.064 (1.009-1.122)	0.023	1.109 (1.015-1.212)	0.022
Baseline age, y	1.011 (0.971-1.053)	0.595	1.012 (0.972-1.054)	0.569
IOP, mm Hg	1.026 (0.89-1.181)	0.727	1.019 (0.882-1.176)	0.801
Baseline VF MD, dB	1.031 (0.959-1.108)	0.414	1.029 (0.957-1.107)	0.435
Intercept (baseline ALCSD _{BMO} /ONHSD _{BMO})	0.998 (0.992-1.004)	0.537	0.997 (0.991-1.004)	0.479

TABLE 5. Hazard Ratios of the Rates of Change of ALCSD_{CSI} and ONHSD_{CSI} and the Covariates for Development of VF Progression Analyzed With Joint Longitudinal and Survival Models

Longitudinal Submodel	ALCSD _{CSI}		ONHSD _{CSI}	
	Coefficient (95% CI)	P Value	Coefficient (95% CI)	P Value
Time, y	9.64 (4.39 to 14.9)	<0.001	8.34 (4.12 to 12.56)	<0.001
Baseline age, y	1.20 (0.14 to 2.26)	0.027	1.23 (0.30 to 2.15)	0.009
IOP, mm Hg	0.01 (−0.47 to 0.49)	0.975	0.42 (0.04 to 0.81)	0.031
Baseline VF MD, dB	−2.46 (−4.19 to −0.73)	0.005	−1.94 (−3.52 to −0.37)	0.016
Time × baseline age	−0.17 (−0.26 to −0.09)	<0.001	−0.14 (−0.21 to −0.08)	<0.001
Time × IOP	0.13 (0.00 to 0.26)	0.049	0.10 (0.00 to 0.2)	0.060
Time × baseline VF MD	0.17 (0.04 to 0.30)	0.011	0.13 (0.02 to 0.23)	0.017
Intercept (baseline ALCSD _{CSI} /ONHSD _{CSI})	336.62 (278.32 to 394.92)	<0.001	168.67 (114.66 to 222.68)	<0.001
Survival Submodel	HR (95% CI)	P Value	HR (95% CI)	P Value
Rate of change of ALCSD _{CSI} /ONHSD _{CSI} (each μm/year)	1.074 (1.016–1.135)	0.011	1.093 (1.013–1.179)	0.022
Baseline age, y	1.012 (0.972–1.053)	0.560	1.013 (0.972–1.055)	0.543
IOP, mm Hg	1.020 (0.885–1.177)	0.784	1.018 (0.884–1.173)	0.804
Baseline VF MD, dB	1.026 (0.954–1.104)	0.484	1.027 (0.955–1.105)	0.473
Intercept (baseline ALCSD _{CSI} /ONHSD _{CSI})	1.000 (0.994–1.006)	0.950	0.998 (0.992–1.005)	0.640

ALCSD and ONHSD were measured with reference to the CSI. Prospective studies are ongoing to measure the longitudinal changes of choroidal thickness in normal individuals and glaucoma patients and delineate the relative contribution of age- versus disease-related choroidal thinning to ALCSD and ONHSD measurements.

Notably, anterior displacement of the anterior LC and the ONH surfaces remained evident in 11.6% and 14.4% of eyes, respectively, even when the CSI reference was adopted. Because glaucoma patients followed-up in this study received IOP-lowering treatment at the discretion of the attending ophthalmologists (the attending ophthalmologists were blind to ALCSD/ONHSD measurements during the study follow-up), it is plausible to observe anterior LC and ONH surface displacement as a consequence of IOP reduction.^{19–21} Alternatively, anterior LC and ONH surface displacement can be age-related independent of the levels of IOP. This is supported by the finding that baseline age was negatively related to the rates of change of ALCSD/ONHSD after controlling for IOP and other covariates in the linear mixed-models (Tables 2, 3). This is also in agreement with a previous study, which showed that for the same degree of glaucomatous damage (measured by VF and OCT RNFL thickness), the ALCSD was shallower in older than younger patients.²⁴ Using finite element modeling, it has been reported that IOP elevation induces circumferential stress on the sclera, resulting in scleral canal expansion, which may pull the LC taut and lead to anterior LC displacement.²⁵ Whether IOP elevation is connected to scleral canal expansion and anterior displacement of the LC and ONH surfaces in glaucoma patients would be an important question for further studies.

The rates of change of ALCSD/ONHSD were highly variable (Fig. 3). We reasoned that eyes with a more rapid posterior deformation of the anterior LC and the ONH surfaces are more likely to develop VF progression. Using joint longitudinal and survival modeling, which computed the HRs of the rates of change of ALCSD/ONHSD for development of VF progression by incorporating subject-specific predictions of the unobserved values derived from the linear mixed-submodel into the survival submodel, we showed that the rates of change of ALCSD and ONHSD were predictive of VF progression independent of the reference (BMO/CSI) used for measurements of ALCSD/ONHSD (Tables 4, 5). Posterior displacement of the anterior LC and ONH surfaces may represent an early biomarker of axonal damage and VF loss in glaucoma patients,

signifying the need of a more intensive treatment regimen and follow-up schedule. Whereas progressive reduction of RNFL thickness and neuroretinal rim area has also been shown to be predictive of VF progression,^{26,27} RNFL and neuroretinal rim loss is irreversible. Progressive posterior displacement of the LC and the ONH surface can be observed prior to detectable RNFL thinning and neuroretinal rim loss.^{8,9,28} Lowering the IOP would be relevant to lessen posterior deformation of the anterior LC and ONH surfaces (as supported by the longitudinal submodel), which would in turn lower the risk of VF progression (as supported by the survival submodel).

Our study is limited in obtaining only six radial B-scans for each eye in each visit. Localized displacement of the anterior LC and the ONH surfaces might have been missed. Nevertheless, we believe data collected from an average of 17.3 visits for each eye over an average of 6.5 years with a total of 15144 B-scans would be sufficient to determine the risk of global rates of change of ALCSD/ONHSD on VF progression. Another limitation is that depth measurements of anterior LC and ONH surfaces are dictated by the location of reference landmark (i.e., BMO/CSI). Change in ALCSD/ONHSD may not necessarily signify deformation of the LC and ONH surfaces. The visibility of the anterior LC surface can be obscured by retinal vasculature, which would hamper the measurement of ALCSD. Yet, there was good to excellent agreement for progressive deformation of the anterior LC and the ONH surfaces (Fig. 2) and the rates of change of ALCSD and ONHSD were both predictive of VF progression. Interpretation of the study results is constrained by the methodology of change analysis and the test-retest variability inherent to SD-OCT and perimetry. The relatively high specificity of the EMGT criteria to define VF progression²⁹ may in part contribute to the temporal disparity in detecting ALCSD/ONHSD changes and VF progression. Finally, the implementation of the joint longitudinal and survival models is currently limited to two-level modeling. Multilevel modeling structures are still under development.

To summarize, longitudinal ALCSD and ONHSD measurements are informative to predict VF progression in glaucoma patients. Given that the rates of change of ALCSD and ONHSD were subject to the influence of visit-to-visit variation of IOP and that faster rates of posterior displacement of the anterior LC and ONH surfaces were associated with a higher risk of VF progression, regular follow-up for measurement of ALCSD and

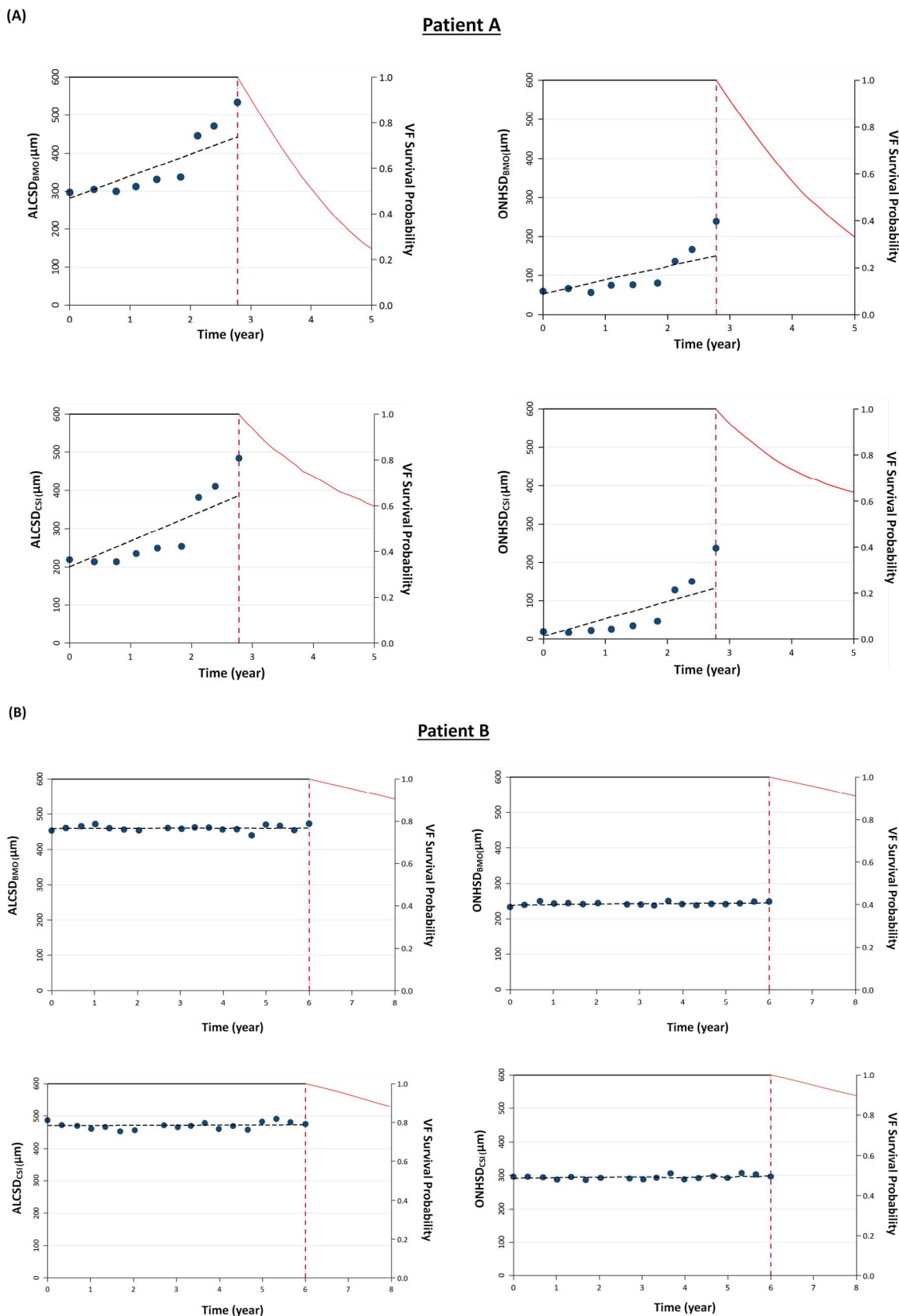


FIGURE 4. Case examples. Conditional VF survival prediction derived from the joint longitudinal and survival modeling in two glaucomatous eyes from two glaucoma patients; one with (A) and one without (B) significant positive trends of the ALCSDBMO (left panel) and ONHSD_{BMO} (right panel) measured with reference to the BMO (upper panel) and the CSI (lower panel). Significantly lower VF survival probabilities were observed for the eye with progressive posterior displacement of the anterior LC and the ONH surfaces (A). “Likely” VF progression (EMGT criteria) was detected in Patient A during the study follow-up. The VF of Patient B showed no progression throughout the study period.

ONHSD is clinically relevant to help determine target IOP and for risk assessment for glaucoma patients.

Acknowledgments

Supported by grants from the Hong Kong Research Grant Council General Research Fund 14101215.

Disclosure: **Z. Wu**, None; **C. Lin**, Carl Zeiss Meditec (F, R), Heidelberg Engineering (R); **M. Crowther**, None; **H. Mak**, None; **M. Yu**, None; **C.K.-S. Leung**, None

References

- Cioffi GA, Robin AL, Eastman RD, Perell HF, Sarfarazi FA, Kelman SE. Confocal laser scanning ophthalmoscope. Reproducibility of optic nerve head topographic measurements with the confocal laser scanning ophthalmoscope. *Ophthalmology*. 1993;100:57-62.
- Leung CK, Cheung CY, Lin D, Pang CP, Lam DS, Weinreb RN. Longitudinal variability of optic disc and retinal nerve fiber layer measurements. *Invest Ophthalmol Vis Sci*. 2008;49:4886-4892.
- Sharma A, Oakley JD, Schiffman JC, Budenz DL, Anderson DR. Comparison of automated analysis of Cirrus HD OCT spectral-domain optical coherence tomography with stereo photographs of the optic disc. *Ophthalmology*. 2011;118:1348-1357.
- Yang B, Ye C, Yu M, Lam DS, Leung CK. Optic disc imaging with spectral-domain optical coherence tomography: variability and agreement study with Heidelberg retinal tomograph. *Ophthalmology*. 2012;119:1852-1857.
- Chauhan BC, Danthurebandara VM, Sharpe GP, et al. Bruch's membrane opening minimum rim width and retinal nerve fiber layer thickness in a normal white population: a multicenter study. *Ophthalmology*. 2015;122:1786-1794.
- Gardiner SK, Ren R, Yang H, Fortune B, Burgoyne CF, Demirel S. A method to estimate the amount of neuroretinal rim tissue in glaucoma: comparison with current methods for measuring rim area. *Am J Ophthalmol*. 2014;157:540-549.
- Wu Z, Xu G, Weinreb RN, Yu M, Leung CK. Optic nerve head deformation in glaucoma: a prospective analysis of optic nerve head surface and lamina cribrosa surface displacement. *Ophthalmology*. 2015;122:1317-1329.
- He L, Yang H, Gardiner SK, et al. Longitudinal detection of optic nerve head changes by spectral domain optical coherence tomography in early experimental glaucoma. *Invest Ophthalmol Vis Sci*. 2014;55:574-586.
- Strouthidis NG, Fortune B, Yang H, Sigal IA, Burgoyne CF. Longitudinal change detected by spectral domain optical coherence tomography in the optic nerve head and peripapillary retina in experimental glaucoma. *Invest Ophthalmol Vis Sci*. 2011;52:1206-1219.
- Hager A, Loge K, Schroeder B, Füllhas MO, Wiegand W. Effect of central corneal thickness and corneal hysteresis on tonometry as measured by dynamic contour tonometry, ocular response analyzer, and Goldmann tonometry in glaucomatous eyes. *J Glaucoma*. 2008;17:361-365.
- Pepose JS, Feigenbaum SK, Qazi MA, Sanderson JP, Roberts CJ. Changes in corneal biomechanics and intraocular pressure following LASIK using static, dynamic, and noncontact tonometry. *Am J Ophthalmol*. 2007;143:39-47.
- Kaufmann C, Bachmann LM, Thiel MA. Intraocular pressure measurements using dynamic contour tonometry after laser in situ keratomileusis. *Invest Ophthalmol Vis Sci*. 2003;44:3790-3794.
- Spaide RF, Koizumi H, Pozzoni MC. Enhanced depth imaging spectral-domain optical coherence tomography. *Am J Ophthalmol*. 2008;146:496-500.
- Johnstone J, Fazio M, Rojananuangnit K, et al. Variation of the axial location of Bruch's membrane opening with age, choroidal thickness, and race. *Invest Ophthalmol Vis Sci*. 2014;55:2004-2009.
- Heijl A, Leske MC, Bengtsson B, Hussein M; for the Early Manifest Glaucoma Trial Group. Measuring visual field progression in the Early Manifest Glaucoma Trial. *Acta Ophthalmol Scand*. 2003;81:286-293.
- Faucett CL, Thomas DC. Simultaneously modelling censored survival data and repeatedly measured covariates: a Gibbs sampling approach. *Stat Med*. 1996;15:1663-1685.
- Crowther MJ, Abrams KR, Lambert PC. Flexible parametric joint modelling of longitudinal and survival data. *Stat Med*. 2012;31:4456-4471.
- Agoumi Y, Sharpe GP, Hutchison DM, Nicoleta MT, Artes PH, Chauhan BC. Lamellar and prelaminar tissue displacement during intraocular pressure elevation in glaucoma patients and healthy controls. *Ophthalmology*. 2011;118:52-59.
- Reis AS, O'Leary N, Stanfield MJ, Shuba LM, Nicoleta MT, Chauhan BC. Lamellar displacement and prelaminar tissue thickness change after glaucoma surgery imaged with optical coherence tomography. *Invest Ophthalmol Vis Sci*. 2012;53:5819-5826.
- Lee EJ, Kim TW, Weinreb RN. Reversal of lamina cribrosa displacement and thickness after trabeculectomy in glaucoma. *Ophthalmology*. 2012;119:1359-1366.
- Lee EJ, Kim TW, Weinreb RN, Kim H. Reversal of lamina cribrosa displacement after intraocular pressure reduction in open-angle glaucoma. *Ophthalmology*. 2013;120:553-559.
- Wakatsuki Y, Shinjima A, Kawamura A, Yuzawa M. Correlation of aging and segmental choroidal thickness measurement using swept source optical coherence tomography in healthy eyes. *PLoS One*. 2015;10:e0144156.
- Sullivan-Mee M, Patel NB, Pensyl D, Qualls C. Relationship between juxtapapillary choroidal volume and beta-zone parapapillary atrophy in eyes with and without primary open-angle glaucoma. *Am J Ophthalmol*. 2015;160:637-647.e1.
- Ren R, Yang H, Gardiner SK, et al. Anterior lamina cribrosa surface depth, age, and visual field sensitivity in the Portland Progression Project. *Invest Ophthalmol Vis Sci*. 2014;55:1531-1539.
- Sigal IA, Yang H, Roberts MD, et al. IOP-induced lamina cribrosa deformation and scleral canal expansion: independent or related? *Invest Ophthalmol Vis Sci*. 2011;52:9023-9032.
- Medeiros FA, Lisboa R, Zangwill LM, et al. Evaluation of progressive neuroretinal rim loss as a surrogate end point for development of visual field loss in glaucoma. *Ophthalmology*. 2014;121:100-109.
- Yu M, Lin C, Weinreb RN, Lai G, Chiu V, Leung CK. Risk of visual field progression in glaucoma patients with progressive retinal nerve fiber layer thinning: a 5-year prospective study. *Ophthalmology*. 2016;123:1201-1210.
- Xu G, Weinreb RN, Leung CK. Optic nerve head deformation in glaucoma: the temporal relationship between optic nerve head surface depression and retinal nerve fiber layer thinning. *Ophthalmology*. 2014;121:2362-2370.
- Artes PH, O'Leary N, Nicoleta MT, Chauhan BC, Crabb DP. Visual field progression in glaucoma: what is the specificity of the Guided Progression Analysis? *Ophthalmology*. 2014;121:2023-2027.